Molecular Crystals and Liquid Crystals

Publication details, including instructions for authors and subscription information:
http://www.tandfonline.com/loi/gmcl20

Revealing the Structure of Focal Conics Cores and their Influence on the Evolution with Temperature: An X-ray Study of Ultra-thin 8CB Films

Jean-Philippe Michel [a], Emmanuelle Lacaze [a], Michel Goldmann [a], Marc Gailhanou [b], Marc de Boissieu [c] & Michel Alba [d]

[a] GPS, Universités Paris, Campus Boucicaut, Paris, France

[b] LURE, Universite Paris Sud, Orsay Cedex, France

[c] LTPCM INPG, Saint Martin d'Hères, France

[d] LLB, CEA-Saclay, Gif-sur-Yvette Cedex, France

Version of record first published: 31 Aug 2006

To cite this article: Jean-Philippe Michel, Emmanuelle Lacaze, Michel Goldmann, Marc Gailhanou, Marc de Boissieu & Michel Alba (2005): Revealing the Structure of Focal Conics Cores and their Influence on the Evolution with Temperature: An X-ray Study of Ultra-thin 8CB Films, Molecular Crystals and Liquid Crystals, 437:1, 99/[1343]-109/[1353]

To link to this article: http://dx.doi.org/10.1080/15421400590954308

Mol. Cryst. Liq. Cryst., Vol. 437, pp. 99/[1343]–109/[1353], 2005

ISSN: 1542-1406 print/1563-5287 online
DOI: 10.1080/15421400590954308

Taylor & Francis
Taylor & Francis Group

Revealing the Structure of Focal Conics Cores and their Influence on the Evolution with Temperature: An X-ray Study of Ultra-thin 8CB Films

Jean-Philippe Michel
Emmanuelle Lacaze
Michel Goldmann
GPS, Universités Paris, Campus Boucicaut, Paris, France

Marc Gailhanou
LURE, Universite Paris Sud, Orsay Cedex, France

Marc de Boissieu
LTPCM INPG, Saint Martin d'Hères, France

Michel Alba
LLB, CEA-Saclay, Gif-sur-Yvette Cedex, France

We have studied by x-ray diffraction the deformations of thin smectic films induced by antagonistic anchorings, as a function of thickness and temperature. The structure of the cores is revealed for thicknesses of the order of 0.15 μm when the deformations are dominated by the presence of the focal conics cores. In a cylindrical geometry imposed by the unidirectional anchoring on the substrate, the cores are tube-shaped rotating grain boundaries (RGB). The spatial extension is of the order of $0.14 \times 0.22\ \mu m^2$, larger than the ones usually proposed in the literature. A drastic evolution of the x-ray scans with temperature is also revealed. It corresponds to a variation of the location of the RGB and is analyzed as the result of a weak variation of the 8CB/air surface tension with temperature.

Keywords: defects; deformations; focal conics; liquid crystals; smectic; temperature; thickness; x-ray diffraction

Address correspondence to Emmanuelle Lacaze, GPS, Universites Paris 7 et 6, UMR-CNRS 75-88, Campus Boucicaut, 140 rue de Lourmel, Paris, 75015, France. E-mail: lacaze@gps.jussieu.fr

The increasing technological interest associated with thin objects requires now a precise understanding of the nature of the defects in thin liquid crystalline films. From a fundamental point of view, the study of liquid crystalline defects in thin films concerns the evolution of soft matter structures in confined geometries. For example, the influence of confinement on the smectic/nematic transition [1,2], which is not understood despite its theoretical importance contrary to the influence of disorder on the smectic/nematic transition [3], could be connected to the presence of defects and their evolution with thickness. We show in this paper that the structure of thin smectic A films can in fact be dominated by the inner structure of focal conics, the so-called core of the focal conics. We also show that the structural evolution with temperature can also be dominated by the presence of focal conics. Focal conics are the more common defects of the smectic A phase and are known since 1922 [4]. However the core structure of these defects still remains mysterious due to the small amount of associated matter. We have then studied 8CB films adsorbed on MoS_2 substrate, deformed through strong antagonistic anchorings at both interfaces but ordered through the presence of a crystallized interface on the single crystal, MoS_2 [5,6]. We had previously demonstrated, combining x-ray diffraction, atomic force microscopy and optical microscopy that, for thicknesses around 0.4 μm, relaxation of the constrains imposed by antagonistic anchorings occurs through the formation of a periodic network of flattened hemicylinders parallel to the substrate (see Fig. 1a) which are 1D focal domains [7]. This order allows x-ray diffraction measurements on smectic films as thin as 0.07 μm. The determination of the focal conics cores as well as their evolution with the temperature has been obtained.

The system is composed of a single crystalline substrate molybdenum disulfide, MoS_2 and the thermotropic liquid crystal 4-n-octyl-4′-cyanobiphenyl, 8CB. MoS_2 natural single crystals are coming from Queensland and are supplied by Ward's (N.Y). MoS_2 is a lamellar compound which surface is composed of ordered sulfur atoms with an hexagonal symmetry ($a_{MoS_2} = 3.16$ Å). The liquid crystal 8CB, smectic in bulk at 25°C, is a product of BDH (Germany) used without any further purification. A 0.1 mol/l solution of 8CB in chloroform is deposited on a freshly cleaved surface of MoS_2. The film's thickness is controlled by spin coating at a speed varying between 1000 and 6000 rpm and is checked by optical microscopy. The sample is annealed at 80°C for thirty minutes to allow formation of the ordered 8CB/MoS_2 interface which imposes a strong planar unidirectional anchoring [8], antagonistic from the homeotropic anchoring at the 8CB/air interface.

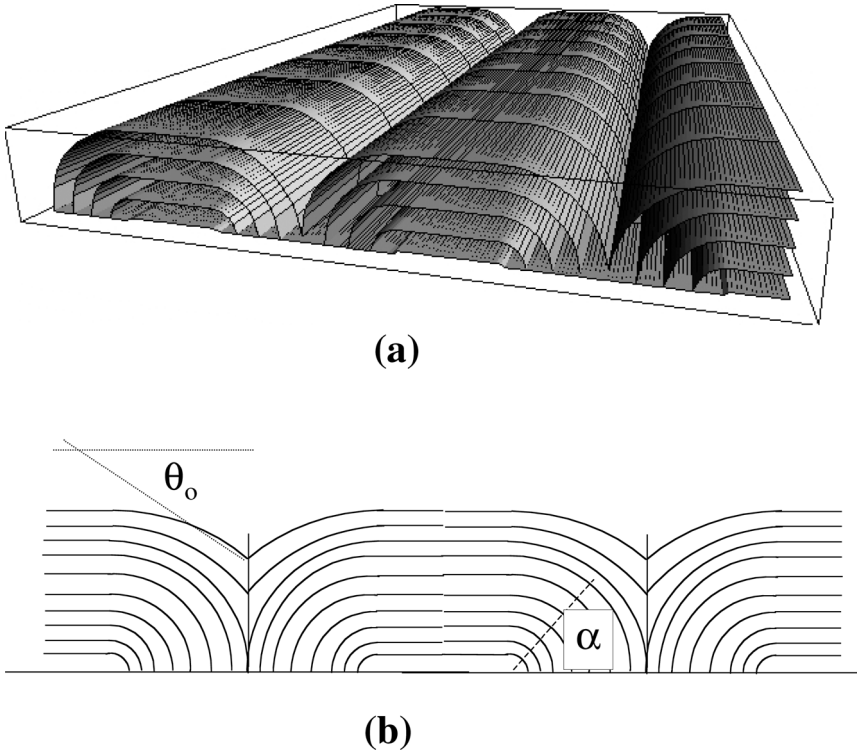

FIGURE 1 (a) Scheme of smectic layers, concentrically stacked into flattened hemicylinders lying flat on the substrate. (b) Cut of the flattened hemicylinders. The curvature wall between neighbouring hemicylinders is represented. It is characterized by the angle at the top, denoted by θ_0. We note α the orientation of the smectic director with respect to the substrate. The proportion of rotating planes varies as $\frac{1}{\cos\alpha}$ between $\alpha = 0^\circ$ and $\alpha = 90^\circ - \theta_0$ and remains constant between $\alpha = 90^\circ - \theta_0$ and $\alpha = 90^\circ$.

X-ray diffraction experiments are performed on D2AM (ESRF, Grenoble, France) and H10 (LURE, Orsay, France) synchrotron beamlines. The energy is fixed at 8 keV, the beam spot is about $50 \times 50\,\mu m^2$ large. The intensity is scanned by a solid-state detector (NaI). We take advantage of the periodic character of the smectic A phase and detect the diffracted intensity at the wave vector modulus q_s corresponding to the 8CB bulk period, $q_S = 0.2\,\text{Å}^{-1}$ [9]. The director being parallel to $\vec{q}_s$, the orientation of the smectic layers is determined by following the orientation of $\vec{q}_s$ and measuring the evolution of Bragg intensity. The director is locked in the azimuthal plane along one of the

permitted anchoring directions on the substrate, so that the wavevector is only flipped from 0° to 90° with respect to the substrate surface [7]. α is defined as the orientation of $\vec{q}_S$ with respect to the substrate surface, such that $\alpha = 0°$ corresponds to layers perpendicular to the substrate and $\alpha = 90°$ corresponds to layers parallel to the substrate.

The Figure 2 presents the evolution of the intensity data when the thickness decreases from 0.45 μm to 0.07 μm, after geometrical corrections and subtraction of the background described elsewhere [7]. In the main frame, the intensity is normalized with respect to the integrated intensity between $\alpha = 0°$ and $\alpha = 85°$. in our set-up, the corrected Bragg intensity is proportional to the number of smectic layers at a given α orientation. The main frame then presents directly the distribution of rotating layers between $\alpha = 0°$ and $\alpha = 85°$, at different thicknesses. The zero intensity between $\alpha = 0°$ and $\alpha = 7°$ is associated with the 8CB critical angle equal to 0.17°. When α becomes smaller than 7°, the incident beam tilt angle becomes smaller than 0.17° and the beam penetration becomes negligible. In the inset, the intensity is normalized with respect to the integrated intensity between $\alpha = 0°$ and $\alpha = 100°$ and is shown around $\alpha = 90°$. It illustrates the presence of a large number of flat smectic layers in the geometry of flattened hemicylinders. The constant number of rotating layers from the orientation perpendicular to the substrate to the parallel one, associated with the presence of quarters of cylinders, is evidenced by a quasi-constant Bragg intensity between $\alpha = 0°$ and $\alpha = 85°$, as shown on Figure 2 in case of thicknesses equal to 0.45 μm. However, starting from a thickness of 0.4 μm, the scans become different.

If we first focus on intensities at α values larger than 40°, two types of variation with α emerge from Figure 2. In the case of thicknesses higher than 0.35 μm, the intensity slightly increases from $\alpha = 40°$ to $\alpha = 85°$ which reflects the presence of focal conics between the flattened hemicylinders, as observed by optical microscopy [7]. In the case of thicknesses smaller than 0.35 μm (0.15 μm and 0.18 μm in Fig. 2), a quasi-constant intensity between $\alpha = 50°$ and $\alpha = 85°$ is consistent with a transformation of focal conics into curvature walls, as proposed in a previous paper [7] (see Fig. 1b). The number of layers increases as $\frac{1}{\cos\alpha}$ between $\alpha = 0°$ and $\alpha = 90° - \theta_0$ and remains constant between $\alpha = 90° - \theta_0$ and $\alpha = 90°$ (Fig. 1b). Figure 2 allows then to deduce an upper limit value for θ_0:θ_0 is greater than 40° for thicknesses of 0.15 and 0.18 μm.

If we now address the intensities at small α values smaller than 40°, the departure from a model of flattened hemicylinders, as the one associated with a thickness 0.45 μm, appears more and more evident on Figure 2 as the thickness decreases. The proportion of layers at

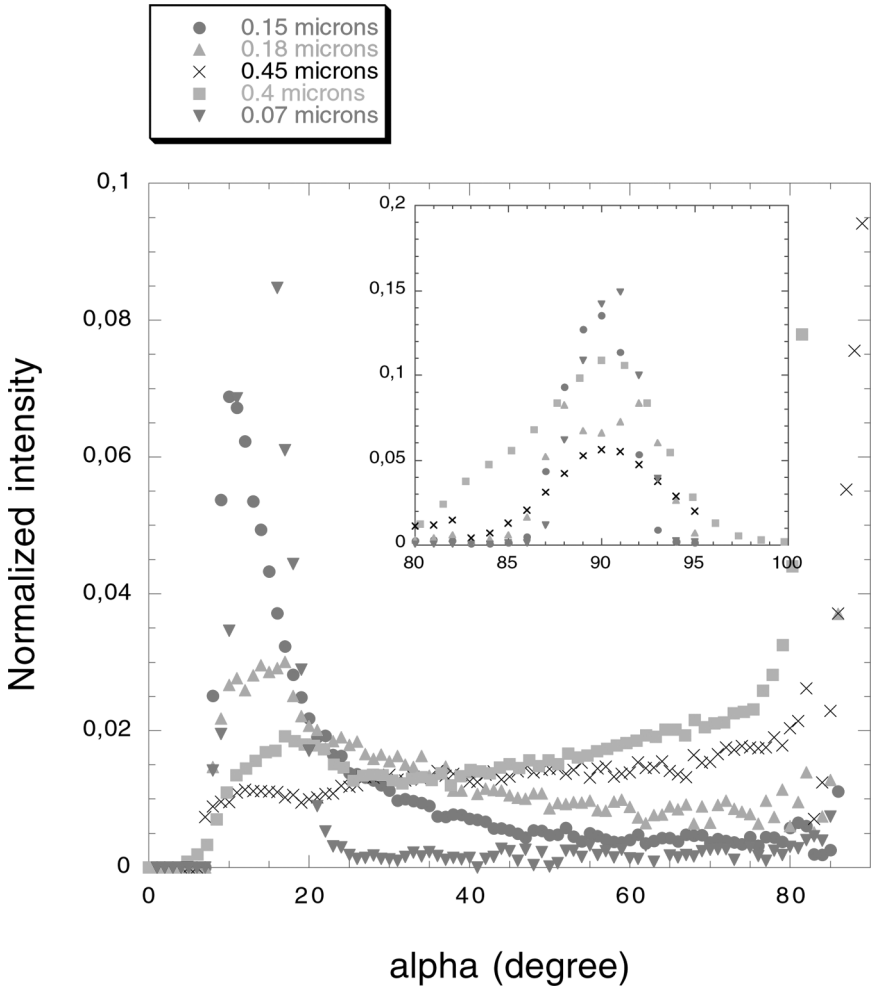

FIGURE 2 Evolution of Bragg intensity with α for different thicknesses (e = 0.45, 0.4, 0.18, 0.15, 0.07 μm), after geometrical correction and subtraction of the background. Intensity is normalized with respect to the integrated intensity between $\alpha = 0°$ and $\alpha = 85°$ in the main frame and with respect to the integrated intensity between $\alpha = 0°$ and $\alpha = 100°$ in the inset.

small α, regarding the proportion at high α, increases as the thickness decreases, leading to layers rotating only between $\alpha = 0°$ to $\alpha = 40°$ for a thickness 0.07 μm. Such an observation can be accounted by the presence of an inner volume in the flattened hemicylinders, with a

form similar to the one shown on Figure 3a, eliminating a larger number of rotating layers at high α than at small α. If radial measurements are performed for the different thicknesses, by varying the azimuthal

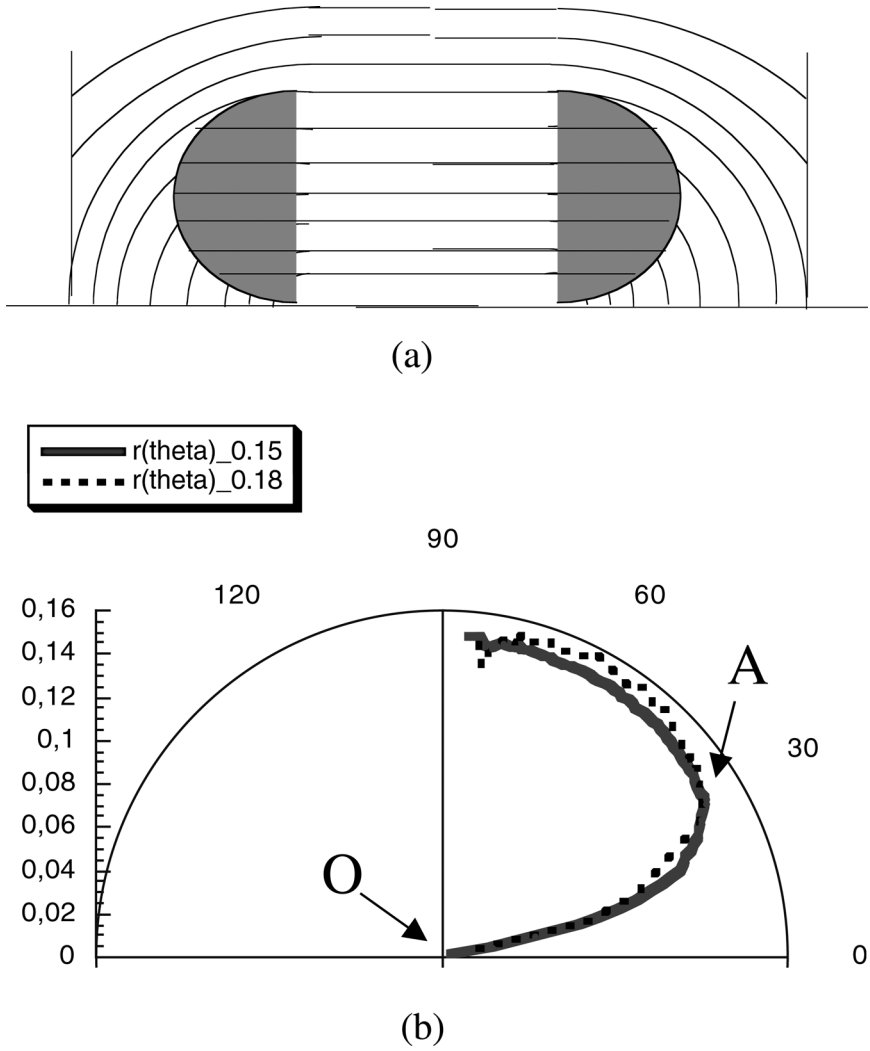

FIGURE 3 (a) Scheme of the inner volume (the RGB is shaded in grey) inside a flattened hemicylinder, eliminating a larger number of rotating layers at high α than at low α. (b) Cut of the RGB in polar coordinates, as deduced from the x-ray data, associated with thicknesses 0.15 μm (line) and 0.18 μm (dotted-line) and the value $\theta_0 = 60°$.

angle with α being fixed, the Bragg intensity appears centered at a constant azimuthal angle, whatever the α value. This result shows that the inner volume also possesses the cylindrical symmetry and allows to show only a cut of the inner volume on Figure 3.

For very small thicknesses, smaller than the inner volume spatial extension, the x-ray signal is dominated by the presence of the inner volume. This is the case of the thickness 0.07 μm, for which only Bragg intensity between $\alpha = 0^\circ$ and $\alpha = 25^\circ$ and at $\alpha = 90^\circ$ is detected (see Fig. 2). This last data demonstrates that the inner volume is constituted by flat layers in contact with rotating ones, through the presence of a rotating grain boundary (RGB), as schematized on Figure 3a.

The Figure 2 then corresponds to the first direct evidence of the core structure of a focal conic, the classical defect of the smectic phase, here associated with a cylindrical symmetry. In case of the thickness 0.07 μm, the basis of the RGB only is present in the film. However, in case of thicknesses 0.15 μm and 0.18 μm, layers rotating up to $\alpha = 90^\circ$ are measured, indicating that the film is slightly higher than the RGB spatial extension. It is then possible to go further and determine the exact form of the RGB, using one of the two spectra associated with thickness 0.15 or 0.18 μm in Figure 2 and the fact that the normalized intensity gives the proportion of rotating layers versus α. Such an interpretation of the data requires to postulate the value of θ_0 associated with the curvature walls between neighbouring flattened hemicylinders. In cases of thicknesses 0.15 and 0.18 μm, θ_0 is known to be larger than 40°. Postulating a value $\theta_0 = 60^\circ$ for these thicknesses, the evolution with α, as obtained through x-ray data, leads to two similar profiles for the RGB (Fig. 3). These profiles have been extrapolated continuously between $\alpha = 7^\circ$ and $\alpha = 0^\circ$ down to O, as shown on Figure 3b. These profiles only slightly evolute, varying the θ_0 value between $\theta_0 = 90^\circ$ and $\theta_0 = 50^\circ$. However, between $\theta_0 = 50^\circ$ and $\theta_0 = 40^\circ$, the profile becomes angulate and different for the two thicknesses 0.15 and 0.18 μm. From these unphysical features we then deduce that θ_0 is greater than 50° and that the real profile of the RGB is the one shown on Figure 3b.

The origin of this volume in the middle of flattened hemicylinders is clear. It avoids the highest curvatures for which the corresponding elastic cost is too high. The dimensions of this volume have consequently no reason to vary with the thickness and, in one hand, its contribution to the evolution of the Bragg intensity with α should diminish as the film thickness increases and become negligible for thick film, as in Figure 2. A calculation of the proportion of rotating layers for a thickness 0.45 μm, taking into account the presence of the profiles of Figure 3b indeed leads to a negligible influence of the RGB.

The focal conic core inside the flattened hemicylinders therefore appears as a half-tube with an elliptical cut of small axis equal to 0.14 μm and of half-large axis equal to 0.11 μm (see Fig. 3b). Such a spatial extension is significantly larger than the distance usually associated with the focal conic cores in the literature, λ the smectic penetration length, equal to some nanometers. The observed spatial extension of the focal conic is in fact related to the replacement of elastic curvature by curvature walls. Such a replacement is known to occur at thickness values varying between 0.1 μm and some microns, depending on the system [7,10,11].

It is now interesting to study the evolution with temperature of such thin and deformed smectic films in order to probe an eventual evolution of the defects. For small thickness (0.15 μm), the evolution of the x-ray scans between $T = 23°C$ to $T = 28°C$ appears very similar to the evolution when the thickness decreases (see Fig. 4a). This demonstrates that the RGB always more dominates the rotation of the smectic layers as the temperature increases. Such a domination, increasing with the temperature, is even observed at higher thickness (0.45 μm, see Fig. 4b), leading to a quasi-disappearance of rotating layers at $\alpha = 50°$. However, in this last case, rotating planes at high α (between $\alpha = 60°$ and $\alpha = 90°$) do not disappear (Fig. 4b). This result has to be associated with the higher thickness of this sample. It shows that the RGB spatial extension increases laterally but not in the direction perpendicular to the substrate. In other words the inner volume of the RGB remains more or less constant as the temperature varies and the extension of the flat layers increases with the temperature, with respect to the rotating ones. This leads to an increasing lateral domination of the RGB with respect to the rotating layers associated with a decreasing of rotating volume, as schematized on Figure 5. This interpretation is supported by the observation of an increasing proportion of flat layers as the temperature increases, which is revealed

FIGURE 4 (a) Evolution of Bragg intensity with α for a thickness 0.15 μm and for different temperatures (T = 23°C, 25°C and 26°C), after geometrical correction and subtraction of the background. Intensity is normalized with respect to the integrated intensity between $\alpha = 0°$ and $\alpha = 85°$ in the main frame and with respect to the integrated intensity between $\alpha = 0°$ and $\alpha = 100°$ in the inset. (b) Evolution of Bragg intensity with α for a thickness 0.45 μm and for different temperatures (T = 23°C, 26°C and 27°C), after geometrical correction and subtraction of the background. Intensity is normalized with respect to the integrated intensity between $\alpha = 0°$ and $\alpha = 85°$ in the main frame and with respect to the integrated intensity between $\alpha = 0°$ and $\alpha = 100°$ in the inset.

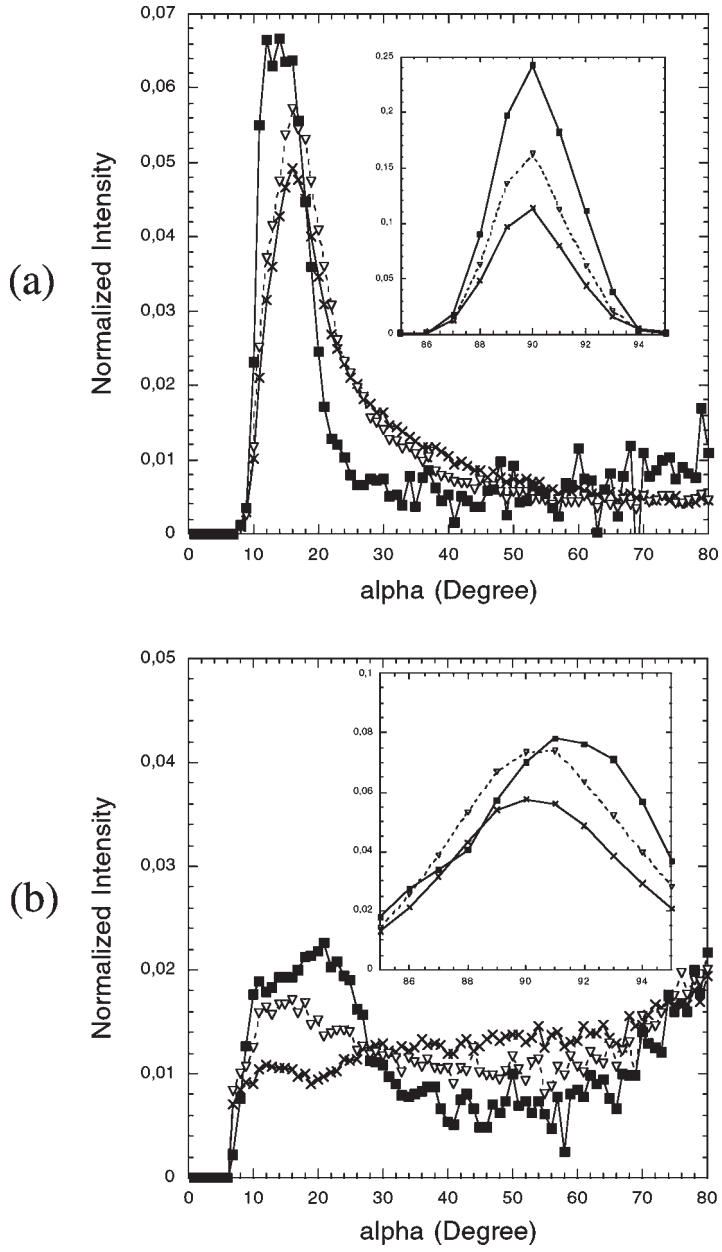

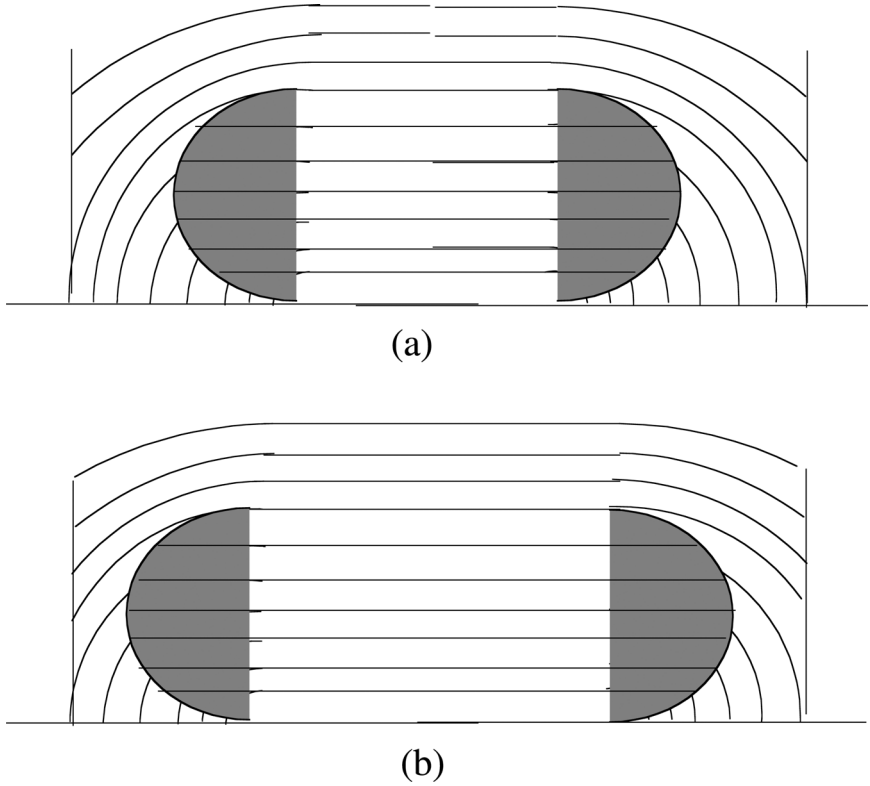

FIGURE 5 Scheme of the evolution of the rotating volume (the RGB is shaded in grey) inside a flattened hemicylinder, associated with the extension of the flat layers which increases between (a) and (b).

by the increasing normalized Bragg intensity close to $\alpha = 90°$ (see the inset of Fig. 4a and Fig. 4b).

This result can be qualitatively understood. The presence of flat layers, unfavorable from the point of view of anchoring on the substrate, is associated with the high cost of 8CB/air curvature which is reduced in case of flattened hemicylinders with respect to normal hemicylinders [7]. Recent measurements of the evolution of the 8CB/air surface tension with the temperature have revealed a weak increase of surface tension with the temperature, in case of smectic 8CB [12]. If such a phenomenon does not occur on the rigid substrate, the energetic cost of the 8CB/air curvature increases with the temperature with respect to the energetic cost of flat layers on the substrate, leading to an increasing number of flat layers with respect to

the rotating ones. This finally leads to an increasing extension of the RGB inside the rotating volume, as experimentally observed. These observations demonstrate how the structure of thin and deformed films can be considerably affected by only small variations of temperature, due to the large influence of surface tensions on the structure of thin films. They also demonstrate how any interpretation of confinement effect is delicate due to the influence of the defects and of their evolution with temperature.

REFERENCES

[1] Iannacchione, G. S. & Finotello, D. (1994). *Phys. Rev. E*, *50,* 4780.
[2] Kralj, S., Zidansek, A., Lahajnar, G., Zumer, S., & Blinc, R. (1998). *Phys. Rev. E*, *57*, 3021.
[3] Bellini, T., Radzihovsky, L., Toner, J., & Clark, N. A. (2001). *Science*, *294*, 1074.
[4] Iannacchione, G. S. & Finotello, D. (1994). *Phys. Rev. E*, *50*, 4780.
[5] Hara, M., Iwakabe, Y., Tochigi, K., Sasabe, H., Garito A. F., & Yamada, A. (1990). *Nature*, *344*, 228.
[6] Lacaze, E., Alba, M., Goldmann, M., Michel, J. P., & Rieutord, F. (2004). *Eur. Phys. J. B*, accepted and published in the Surfaces and Interfaces section.
[7] Michel, J. P., Lacaze, E., Alba, M., de Boissieu, M., Gailhanou, M., & Goldmann, M. (2004). *Phys. Rev. E*, accepted and published.
[8] Lacaze, E., Michel, J. P., Goldmann, M., de Boissieu, M., Gailhanou, M. & Alba, M. (2004). *Phys. Rev. E*, *69*, 041705, 1–8.
[9] Davidov, D., Safinya, C. R., Kaplan, M., Dana, S. S., Schaetzing, R., Birgeneau, R. J., & Litster, J. D. (1979). *Phys. Rev. B*, *19*, 1657.
[10] Williams, C. E., Kleman, M. & Physique, J. (1975). *Colloque C1*, supplement au nb 3, tome *36*, 315–320.
[11] Blanc, C. & Kleman, M. (1999). *Eur. Phys. J. B*, *10*, 53.
[12] Tintaru, M., Moldovan, R., Beica, T., & Frunza, S. (2001). *Liquid crystals*, *28*, 793.